The effect of defects on tensile strength of the continuous steel casting products

Vpliv napak na natezno trdnost kontinuirno ulitih jeklenih proizvodov

Mirko Gojić[1,*], Ladislav Lazić[1], Stjepan Kožuh[1], Ladislav Kosec[2]

[1]University of Zagreb, Faculty of Metallurgy, Aleja narodnih heroja 3, 44103 Sisak, Croatia
[2]University of Ljubljana, Faculty of Natural Sciences and Engineering, Aškerčeva 12, 1000 Ljubljana, Slovenia

*Corresponding author. E-mail: gojic@simet.hr

Received: May 23, 2011 **Accepted:** October 6, 2011

Abstract: The goal of this paper is to determine the influence of defects on tensile strength of continuous casting steel products made from low alloy Mn-V steel. The microstructure was determined by optical microscopy and scanning electron microscopy. The composition of non-metallic inclusions were determined by energy dispersive X-ray spectroscopy. The microstructural analysis has shown that there are significant differences between the microstructure near the surface and in the central zone of the round cross-section. It was found that a significant decrease in tensile strength can be correlated the presence of alumina and sulphide inclusions as well as dendritic structure.

Povzetek: Namen članka je določiti vpliv napak na natezno trdnost kontinuirno ulitih jeklenih proizvodov, izdelanih iz Mn-V malooglјičnega jekla. Mikrostruktura je bila analizirana z optičnim mikroskopom in vrstičnim elektronskim mikroskopom. Kemična sestava nekovinskih vključkov je bila opredeljena z energijsko disperzijsko spektroskopijo rentgenskih žarkov. Mikrostrukturna analiza je pokazala občutno razliko med mikrostrukturo blizu površine in tisto v centralni coni prečnega prereza. Ugotovili smo, da je občuten padec natezne trdnosti v korelaciji s prisotnostjo aluminatnih in sulfidnih nekovinskih vključkov in tudi z dendritsko strukturo.

Original scientific paper

Key words: low alloy steel, solidification, non-metallic inclusions, continuous casting
Ključne besede: maloogljično jeklo, strjevanje, nekovinski vključki, kontinuirno litje

Introduction

It is known that continuous casting of steels involves many physical phenomena (fluid flow, heat transfer, solidification etc.).[1–4] The flow of liquid steel inside the strand influences the quality of solidified steel, solidification structure, inclusion distribution and segregation.[5] One of the factors in connecting the quality of steel products is the cleanness of the steel, which refers to the non-metallic inclusion content in the steel. The presence of the defects from the steelmaking process can initiate a local weakness of the steel and its failure during application. Among others, low alloy steels are used commonly for oil country tubular goods (OCTG). The main reasons for this application are excellent hardenability, high strength, good toughness and high resistance to sulphide stress corrosion cracking (SSCC) as a form of hydrogen embrittlement.[6] Since these steels are used under complex loads, their defects (especially non-metallic inclusions) should be strictly controlled to decrease their negative effects.[7] Limitation of non-metallic inclusions and reduction of centreline segregation have a very important role in increasing the resistance of low alloy steels to hydrogen induced cracking (HIC) and sulphide stress cracking (SSC). Non-metallic inclusions in steel are originated from deoxidation, reoxidation, segregation and chemical reactions with the refractories.[8, 9]

Since mechanical properties and resistance to corrosion are influenced by the presence of defects in the steel, the objective of this paper is to establish the type, size and distribution of non-metallic inclusions and dendritic structure across the cross-section of the continuous casting products, as well as their impact on tensile strength. The obtained results will serve in the subsequent thermal stress analyses, questioning whether the temperature differences, appearing across the cross-section of the products heated in the rotary-hearth furnace, lead to thermal stresses which exceed the tensile strength of the final products and cause stress cracks in the structure. The investigation methodology consists of testing the tensile strength of the specimens taken at different places of cross-section of cast products, as well as examinations of the microstructural features of steel structure and defects on the tested tensile specimens using optical microscope (OM) and scanning electron microscope (SEM) methods, respectively.

Materials and methods

The cast steels for this investigation were produced in an electric arc furnace. The range of composition of the steel under investigation is given in Table 1. As can be seen, the steel grade corresponds to the low alloy Mn-V steel. The molten steel is continuously cast in the round cross-section with the diameter of 410 mm. Specimens for tensile tests were machined from the round cross-section in accordance with ASTM standards.[10] The specimens were taken from the mid-thickness location in two series all over the cross-section, starting from the surface, across the central zone to the opposite end (Figure 1). In this sequence, the specimens were tested at test temperatures from 100 °C up to 650 °C, with the step of 50 °C. The specimens were elongated to fracture on Zwick 50 kN tensile testing machine. The specimens for metallographic analysis were grinded and polished. After that the specimens were etched by a nital solution consisting of 5 % nitric acid in ethyl alcohol. Metallographic analysis was carried out on both etched and non-etched samples. Microstructural examination was carried out using an optical microscope (OM) and scanning electron microscope (SEM) equipped with energy dispersive X-ray spectrometry (EDX). EDX unit was used for the spot aimed chemical X-ray microanalysis. Fraction of inclusions was determined by quantitative metallogra-

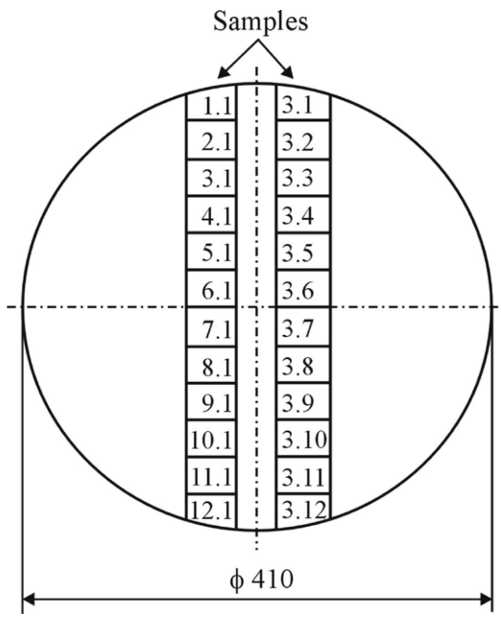

Figure 1. Schematic illustration of samples taken for the tensile test.

Table 1. Chemical composition of the investigated steel in mass fractions, *w*/%

C	Mn	Si	Al	V	P_{max}	S_{max}
0.30–0.34	1.15–1.30	0.15–0.35	0.02–0.04	0.15–0.18	0.025	0.025

phy method using optical microscopy Olympus BX61. There measurements were made on specimens from the outer and inner regions. Fractographic analysis of tensile test specimens after fracture was carried out using SEM.

RESULTS AND DISCUSSION

In order to remove the flawed layer produced by polishing and in order to reveal the microstructural details, the specimen surfaces were etched by the nital solution. Optical and SEM micrographs of the etched specimens at surface and central zone of the round cross-section are shown in Figures 2, 3 and 4. The OM and SEM micrographs of the specimens near to the surface (Figures 2a and 3a) shows the pearlite-ferrite microstructure consisting of ferrite within the eutectoid structure. Ferritic grains are mostly surrounded by

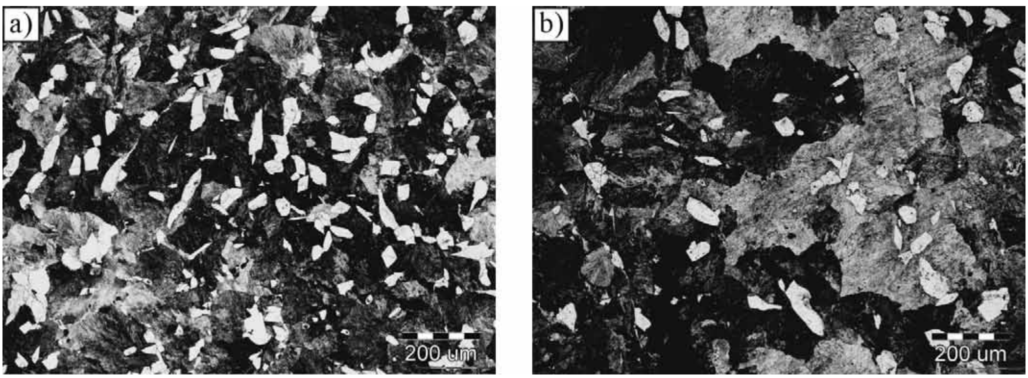

Figure 2. Microstructures of the steel product near the outer surface (a) and in the central zone (b) obtained using OM on specimens etched by nital solution.

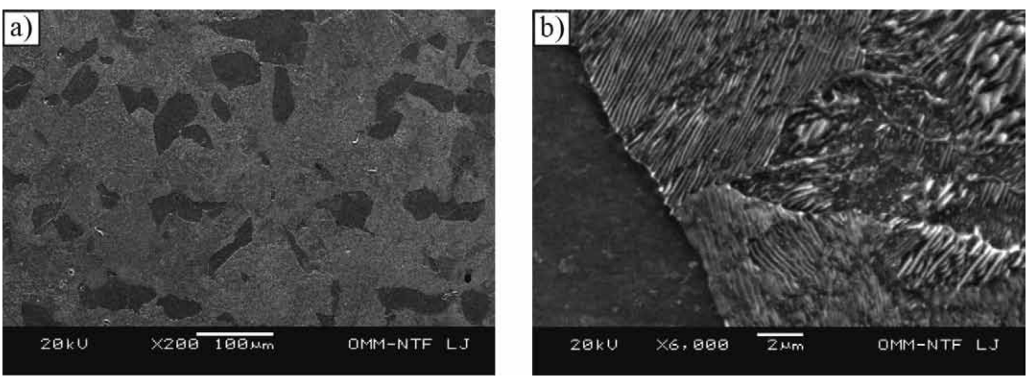

Figure 3. Microstructures of the steel product near the outer surface obtained using SEM at different magnifications.

the pearlitic grains. This pearlite can be characterized as lamellar (Figures 3b and 4b). The specimens in the central zone (Figures 2b, 3b and 4) also have pearlite-ferrite microstructure comprising randomly-oriented grains, characteristic for a central equiaxed zone. The grains are of different size and form. Grains are larger compared with the surface samples. The coarse-grain structure resulted from the slow cooling rate at the casting core. The grain

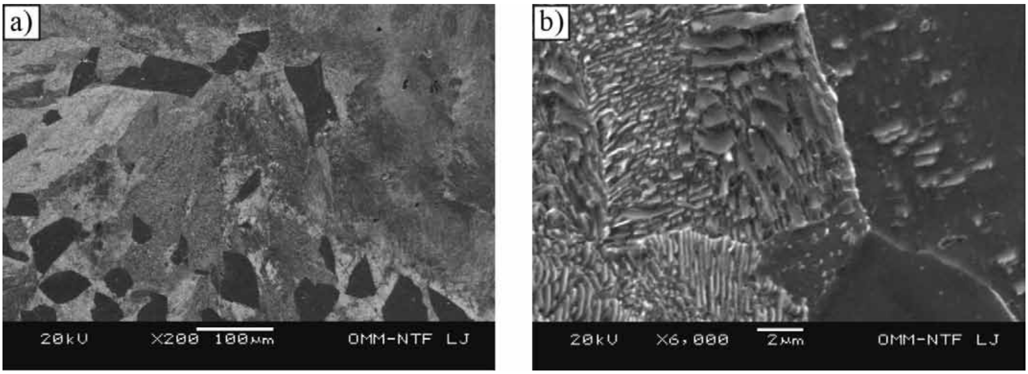

Figure 4. Microstructures of the steel product in the central zone obtained using SEM at the different magnification.

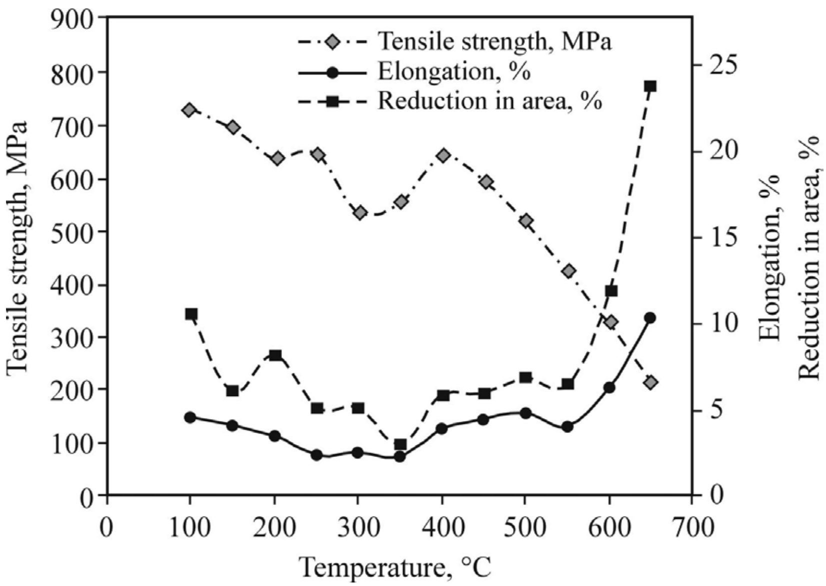

Figure 5. Variations of the tensile strength, elongation and reduction in area with the testing temperature.

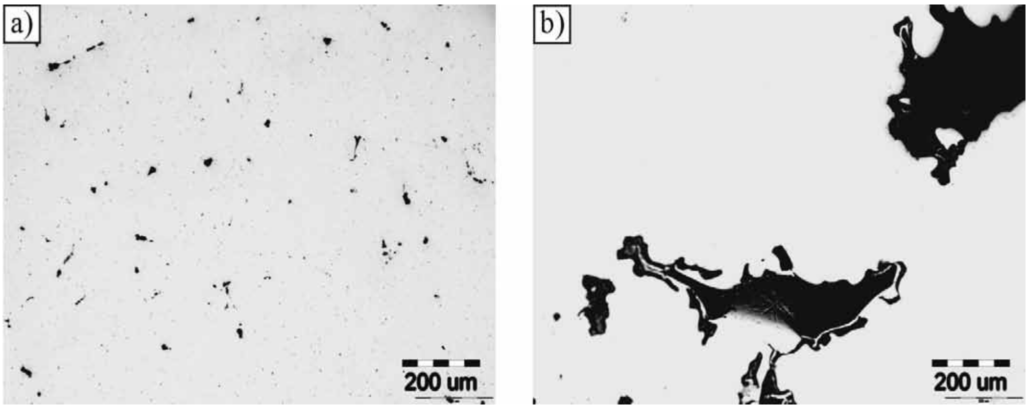

Figure 6. Microstructures of the steel product near the outer surface (a) and in the central zone (b) obtained using OM on non-etched specimens.

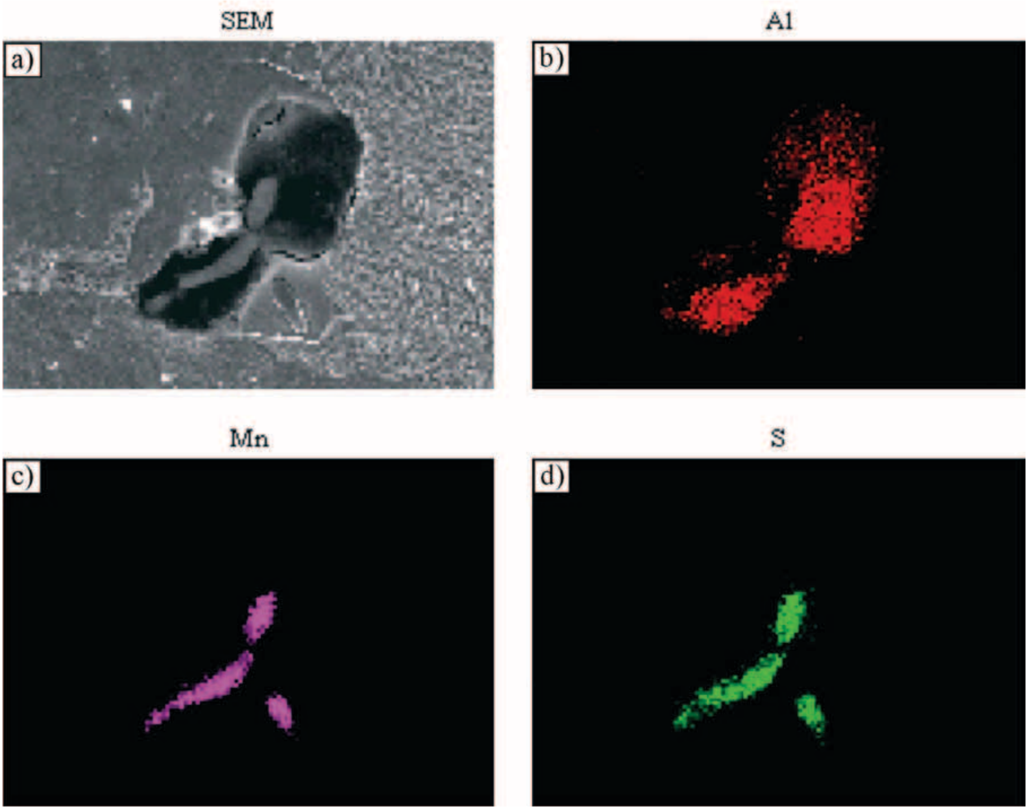

Figure 7. Microstructures of the steel product at the ferrite/pearlite interface obtained using SEM (a) and elemental maps for aluminium (b), manganese (c) and sulphur (d).

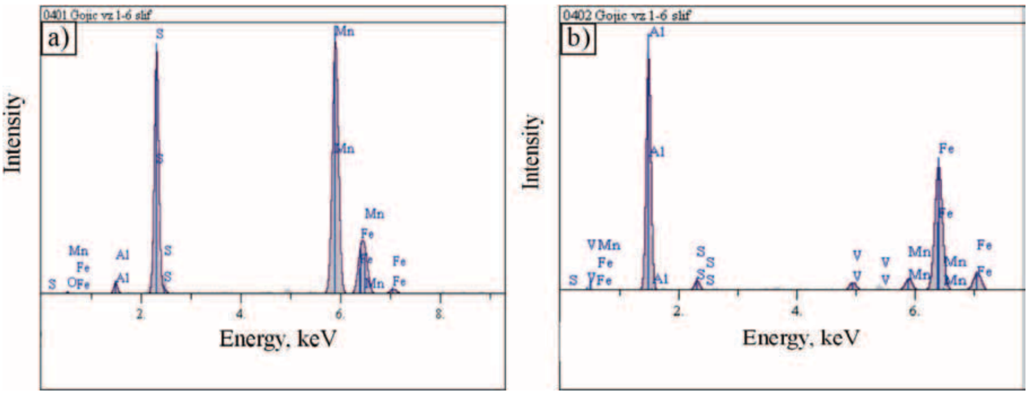

Figure 8. EDX spectra of particles enriched with sulphur (a) and aluminium (b) at the ferrite/pearlite interface shown in Figure 7a.

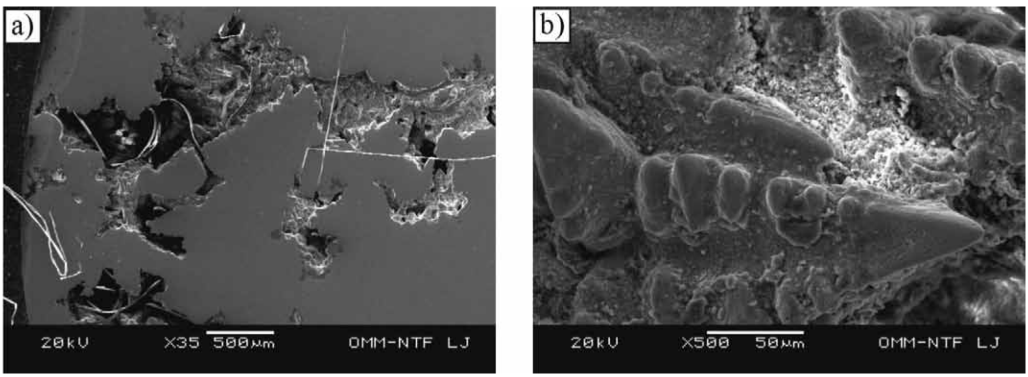

Figure 9. Microstructures of the steel product in the central zone obtained using SEM at different magnifications, 1st position.

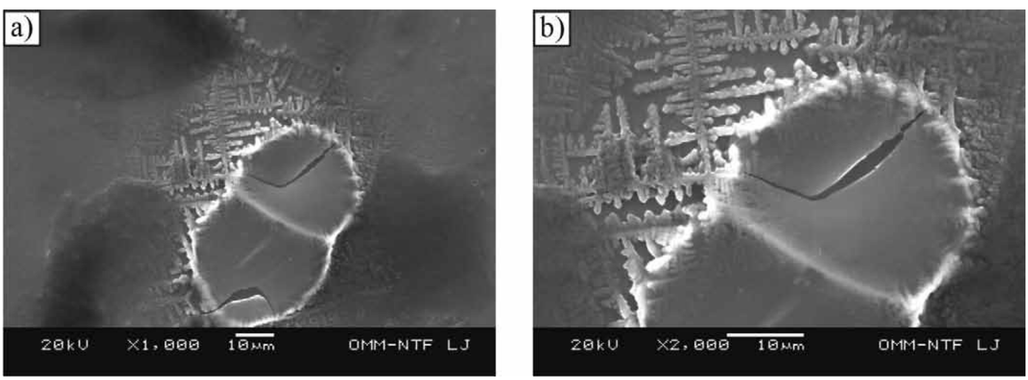

Figure 10. Microstructures of the steel product in the central zone obtained using SEM at different magnifications, 2nd position.

boundaries between ferrite and pearlite are clearly visible (Figures 3b and 4b).

The values of tensile strength are obtained by conducting tensile stress-strain tests at elevated temperatures. Figure 5 shows the influence of temperature on tensile strength. It was found that tensile strength decreases with increasing temperature. However, for specimens cut from the central zone of the round cross-section, the hot tensile strength suddenly dropped in the temperature range from 250 °C to 350 °C. The reason of this phenomenon may be only in the metallurgical cleanness of the cast steel.

The optical, SEM and EDX analysis of the specimens at surface and core of the cast steel are shown in Figures 6, 7, 8, 9 and 10. Figure 6a shows the presence of inclusions on non-etched surface. Fine inclusions distributed uniformly at surface were found. There is no important porosity. In the Figures 6b, 7, 8, 9 and 10 many inclusions and dendritic structure in the central part of the round cross-section may be seen. Numerous inclusions are probably segregated between dendrites. Fraction of inclusions into outer regions of the cast steel was 1.55 %, while the fraction of inclusion into core of the cast steel was 2.50 %.

The high deflection region of hot tensile strength ranging from 250 °C to 350 °C (Figure 5) can be connected with microstructural change. It is likely to be attributed to the presence of non-metallic inclusions (Figures 6–9a) and coarser dendritic structure with a small proportion of equiaxed grains in the core of continuous cast products (Figures 9b and 10).

The inclusions segregate in the inter-dendritic regions of the solidifying steel because they were not able to float out. They formed in molten steel before the solidification or after beginning of solidification in interdendritic regions. The composition of inclusions was analysed by EDX-method (Figure 8). The EDX-spectrum shown in Figure 8a illustrates the peaks of manganese and sulphur, while Figure 8b shows peaks of aluminium and iron. Thus the inclusions have complex composition (alumina and sulphide). The formation of alumina and sulphide inclusions as the result of deoxidation and desulphurization processes can be described by the following reactions [11]:

$$3[O] + 2[Al] \rightarrow (Al_2O_3) \quad (1)$$

$$(MnO) + [FeS] \rightarrow (MnS) + (FeO) \quad (2)$$

Alumina inclusions generated by reaction between the dissolved oxygen and the added aluminium deoxidant are typical deoxidation inclusions in steels. They are hard and non-deformable and tend to form oxide clusters. Angular aluminium oxide inclusions are probably more deleterious than particles with rounded shapes. Small sulphide inclusions can be harmful, especially for steel used for exploitation of oil and natural gas. Manganese sulphide can decrease the plasticity of steel during rolling due to its low melting temperature.

According to their composition, the inclusions might be endogenous, i.e. product of the deoxidation and precipitation during cooling and solidification. Inclusions being formed during the solidification process in interdendritic spaces, termed secondary inclusions, may be either pushed by the advancing solid-liquid interface, i.e. by the thickening dendrite arm, or trapped within the dendrite arm as the solid front moves (for example alumina). The structure, distribution of segregations and non-metallic inclusions, as well as other qualitative characteristics, differ widely between individual cross-sections because the shape and size of the cross-section of continuous castings influence the crystallization process. The manner of final meetings of the crystallization fronts depends on the shape of the casting (mould) cross-section. For the circular or square cross-section the crystallization fronts meet in one point and for the rectangular cross-section in one line. The latter is more favourable in view of the distribution of non-metallic inclusions and segregations.

The fracture surfaces reflect the changes in microstructure. Scanning electron fractograph (Figure 11) of the broken surface specimen near to the surface shows mostly the mixture of ductile and transgranular cleavage fracture surfaces. Ductile fracture is a result of decohesion along the non-metallic inclusion/matrix interfaces. This fracture is characterized by void nucleation, growth and coalescence. Even at small plastic strains the non-metallic inclusions will be released from the ductile matrix and in that way they cause the nucleation of voids, which grow with increasing load. Some of cleavage facets were initiated by inclusions (Figure 11b). Obtained microstructural results in the central zone of the steel products (Figures 9 and 10) are confirmed by fractographic analysis. Scanning electron fractograph of the broken core specimen shows the predominant dendritic structure (Figure 12) which serves as an initiation centre of cleavage. As it can be seen, specimens in the central zone show interdendritic fracture morphology (Figures 12a and 12b) with primary and secondary dendrite arms (Figures 12c and 12d). Primary columnar dendrite arm spacing is around 450 μm, while the secondary columnar dendrite arm spacing ranges from 10 μm to 100 μm, which is according to the results of investigation by Fujda et al.[12]

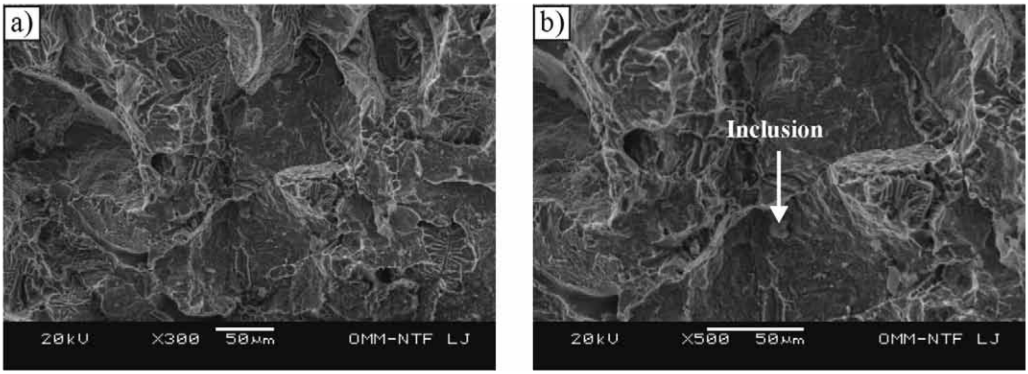

Figure 11. SEM micrographs of fracture surface near the surface of the round cross-section at different magnifications.

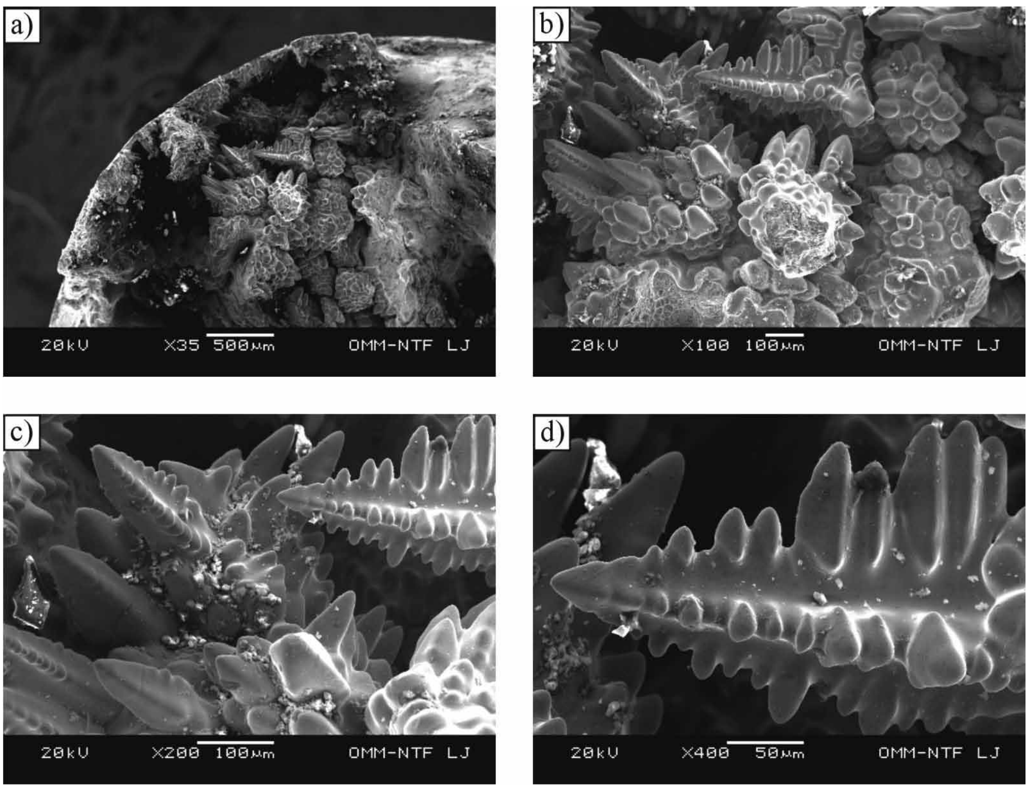

Figure 12. SEM micrographs of fracture surfaces in the central zone of the round cross-section at different magnifications.

It is known that solidification grain structure of the cross-section of continuous casting consists of an outer equiaxed zone comprising fine, randomly-oriented grains, an intermediate columnar zone comprising elongated, oriented grains and a central equiaxed zone, again comprising randomly-oriented grains. Thus the steel solidification in casting is dendritic. Each equiaxed grain contains one dendrite, with many dendrite arms. Many secondary dendrite arms grow from a single primary dendrite arm. Due to the anisotropy of properties, such as solid/liquid interface energy and growth kinetics, dendrites will grow in a preferred crystallographic direction that is closest to the heat flow direction, whereas cells grow with their axes parallel to the heat flow direction without regard to the crystal orientation. The columnar grains always grow out from the mould (which is the heat sink) in direction which is opposite to that of the heat flow, while equiaxed growth takes place in a supercooled melt which acts as their heat sink. Thus, the growth direction and the heat flow direction are the same in equiaxed growth. The grain size often, but not always, decreases with increasing cooling rate. Fineness of the dendritic structure, the primary and secondary arm spacings, always decreases with increasing cooling rate. The characteristic of the continuous casting is a high solidification rate in the direction of casting (mould) centre. As a general rule, the characteristic of continuous casting is a high solidification rate in the direction of the mould centre.

Conclusions

Results show that tensile strength of the low alloy Mn-V continuous casting steel decreased by increasing temperature testing. Characteristic decreasing of tensile strength in the central zone of continuously cast round cross-section with diameter of 410 mm is the result of microstructural changes. Different microstructures are observed depending on the depth under the surface of the round cross-section. Central zone samples showed higher content of non-metallic inclusions and dendritic structure. These inclusions are alumina and sulphides. They are the results of chemical reactions during deoxidation and solidification of the steel.

References

[1] Yasuda, H., Toh, T., Iwai, K., Morita, K. (2007): Recent progress of EPM in steelmaking, casting, and solidification processing. *ISIJ International*, *47*, pp. 619–626.

[2] De Barcellos, V. K., Da Silva Gschwenter, V. L., Kytönen, H., Dos Santos, C. A., Spim, J., Louhenkilpi, S., Miettinen, J.

(2010): Modelling of Heat Transfer, Dendrite Microstructure and Grain Size in Continuous Casting of Steels. *Steel Research Int.*, *81*, pp. 461–471.

[3] KITAMURA, S. (2010): Importance of Kinetic Model in the Analysis of Steelmaking Reactions. *Steel Research Int.*, *81*, pp. 766–771.

[4] DOMITNER, J., KHARICHA, A., GRASSER, M., LUDWIG, A. (2010): Reconstruction of Three-Dimensional Dendritic Structures Based on the Investigation of Microsegregation Patterns. *Steel Research Int.*, *81*, pp. 644–651.

[5] JAVUREK, M., BARNA, M., ROCKENSCHAUB, K., LECHNER, M. (2008): Flow Modelling in Continuous Casting of Round Bloom Strands with Electromagnetical Stirring. *Steel Research Int.*, *79*, pp. 617–626.

[6] GOJIĆ, M., KOSEC, B., ANŽEL, I., KOSEC, L., PRELOŠĆAN, A. (2007): Hardenability of steels for oil industry. *Journal of Achievement in Materials and Manufacturing Engineering*, *23*, pp. 23–26.

[7] GOJIĆ, M., KOSEC, L., MATKOVIĆ, P. (2003): Embrittlement damage of low alloy Mn-V steel.*Engineering Failure Analysis*, *10*, pp. 93–102.

[8] THUNMAN, M., SICHEN, D. (2008): Origins of Non-metallic Inclusions and their Chemical Development during Ladle Treatment. *Steel Research Int.*, *79*, pp. 124–132.

[9] PFEILER, C., THOMAS, B. G., WU, M., LUDWIG, A., KHARICHA, A. (2008): Solidification and Particle Entrapment during Continuous Casting of Steel. *Steel Research Int.*, *79*, pp. 599–607.

[10] ASTM, A370-94. Standard test method and definitions for mechanical properties of steel products, ASME, New York, 1994.

[11] GOJIĆ, M., KOŽUH, S., KOSEC, B. (2010): SEM and EDX analysis of continuous casting of steel. *Acta Metallurgica Slovaca Conference-special issue*, *15*, pp. 235–237.

[12] FUJDA, M., LONGAUEROVÁ, M. (2006): Morphology of fine surface cracks on low carbon steel CC slab enriched by copper. *Acta Metallurgica Slovaca*, *12*, pp. 243–249.